Bridging the Gap: Matching Data from Low-Cost Mobile Sensors and Satellite for Urban Heat Island Research. A case study in Padua, Italy.

Carlo Zanetti [1], Lisa Rubert [2], Massimo De Marchi [3], Salvatore Eugenio Pappalardo [4]

[1] Human Rights Centre "Antonio Papisca", University of Padua, Italy – carlo.zanetti@unipd.it
[2] School of Engineering, Department of Civil Environmental and Architectural Engineering, University of Padua, Italy - lisa.rubert.1@studenti.unipd.it
[3] Advanced Master in GIScience, Department of Civil, Environmental and Architectural Engineering, University of Padua, Italy - massimo.de-marchi@unipd.it
[4] Laboratory GIScience and D4G, Department of Civil, Environmental and Architectural Engineering, University of Padua, Italy – salvatore.pappalardo@unipd.it

Keywords: Urban Heat Island, Land Surface Temperature, Heat Waves, Climate Adaptation, Extreme Heat, Landsat, Low-Cost Device.

Abstract

In recent decades, the phenomenon of urban heat islands has intensified due to the increased frequency, magnitude, and duration of extreme weather and climate events. The study of urban microclimates plays a crucial role in implementing actions to reduce thermal stress caused by urban heat islands. Typically, urban heat islands are identified through thermal satellite images (e.g. Sentinel, Landsat). However, these tools are inadequate for detecting heat islands at an appropriate spatial and temporal scale. Furthermore, satellite images do not measure air temperature but rather the land surface temperature, which is not directly usable to estimate thermal stress on the population. To address this issue, we explored, during Summer 2023 in Padua, the feasibility of using a low-cost sensor (MeteoTracker©) to map urban heat islands, to assess spatial relationships with impermeable surfaces, and to investigate potential correlations with land surface temperature. Over an overall mobile mapping of 540 km, on average, air temperature is 1 °C higher in impermeable areas compared to permeable ones. Confirming this, a 0.1 increase in Normalized Difference Vegetation Index (NDVI) corresponds to a temperature decrease of 0.23 °C in the afternoon and 0.3 °C in the night. Moreover, a positive relationship was found between Land Surface Temperature (LST) and air temperature: an increase of approximately 2 °C in LST for every 1 °C increase in air temperature. This study lays the foundation for further research on urban heat islands, integrating satellite and ground data for the development of high-resolution adaptation actions.

1. Introduction

1.1 Urban Heat Island Phenomenon

Recent studies have identified Europe as a major hotspot for heat waves, defined as prolonged periods of extreme heat caused by climate change (Rousi et al., 2022). Heat waves will increase in frequency, magnitude and duration in the next decades (IPCC, 2021) This increase in heat extremes is exacerbated in the urban environment due to the Urban Heat Island (UHI) effect (Oke, 1973) which is an urban area where temperatures are higher than the surrounding rural environment. The factors contributing to UHI are many and interrelated. A primary contributor to the UHI effect is soil sealing and the absence of vegetation. Vegetation serves as a natural air conditioner due to shadow as well the cooling effect of the evapotranspiration process (Grigoras and Urițescu, 2019; Koko et al., 2021). The albedo effect also contributes to UHI, especially during the night, where dark urban materials such as asphalt release heat (Morini et al., 2018). Urban morphology also contributes to limit heat exchanges, with the so-called Urban Canyon Effect, where high buildings do not allow proper ventilation (Giannopoulou et al., 2010). Another factor contributing directly to urban heat is anthropogenic heat, like endothermic cars and domestic heat releases.
More than 55% of global population lives in urban areas, and in 2050 this percentage will increase to 68%. (UN, 2019), so it is urgent to implement adaptation actions to mitigate the UHI phenomenon.
The impacts of extreme heat on health are enormous. The heatwaves that hit Europe in 2003, caused around 70,000 deaths (Robine et al., 2008), while in 2022 summer it is estimated an excess mortality of 61.000 person, 18.000 of which in Italy (Ballester et al., 2023).
Nature Based Solution (NBS), such as urban parks, trees, green roofs and water infrastructures can contribute to mitigate the adverse effect on health of UHIs. To maximize the heat mitigation potential of NBS, it is crucial to create a high-resolution geodatabase detailing the urban environment's land cover and microclimate. High-resolution temperature data, both temporally and spatially, is crucial for identifying suitable NBS interventions and determining their optimal implementation locations.

1.2 Citizen Science: Linking Pixel and People

The high variability of microclimates within urban environments, and the sparse distribution of weather stations in most cities, leads to a notable scarcity of information regarding urban microclimates. To tackle this challenge, UHI studies commonly employ Land Surface Temperature (LST) as a means to monitor urban temperatures. While this approach offers high spatial resolution, it often falls short in temporal resolution. Additionally, the presence of clouds doesn't allow the acquisition of temperature data.
To address this challenge, employing low-cost devices for air temperature monitoring can notably boost data acquisition by involving citizens in data collection efforts. Installing such

weather stations on bikes or cars offers a practical means to gather widespread and real-time temperature data across urban areas. This approach aligns with the concept of Citizen Science, wherein non-specialist individuals, often ordinary citizens, participate in scientific research by collecting data, observing natural phenomena, or analysing data (Dickinson et al., 2010). This participation of "non-expert" citizens is usually coordinated by scientists or professional organizations to address scientific or environmental issues.
Involving citizens is crucial when it comes to addressing and managing the local impacts of climate change for several reasons. First of all, by actively involving citizens we can increase awareness and understanding of the phenomenon and its impacts; this is essential to motivate personal and collective actions (Robinson et al., 2018). In fact, participation and information stimulate citizens' desire to promote energy saving, the reduction of personal carbon emissions and the promotion of environmental and sustainable policies, putting pressure on decision-makers to take more effective measures to mitigate climate change (Rubio-Iglesias et al., 2020).
Bicycles equipped with sensors capable of measuring various air pollutants, humidity and air temperature allows to cover as many parts of the city as there are moving devices, ensuring abundant and almost daily data availability. The advantages deriving from this type of choice are various, for example: stimulating cyclists to choose more temperate roads and routes; help particularly sensitive individuals to avoid hot areas at certain times of the day, or choose cooler areas of the city; help local administrations in making decisions from an urban planning point of view, encouraging the presence of parks and green areas; help research organizations collect more data to better understand the UHI phenomenon.
For the following study, the MetroTracker© mobile device was used, a sensor capable of sampling the air based on fixed frequency, measuring temperature and relative humidity.

1.3 Objectives

The overall purpose of this study is to investigate the thermal conditions of the air in different areas of the city of Padua, at different times (afternoon and night) and under different meteorological situations, through the use of the low-cost mobile device MeteoTracker©. The first phase of the research involves the analysis of data collected in the urban area of Padua from July to September 2023, with the aim of identifying and mapping the UHIs in the surveyed areas. In particular, a correlation analysis was carried out between air temperature and land use and the Normalized Difference Vegetation Index (NDVI).
In the second part of the research, the relationship between air temperature and the Land Surface Temperature (LST) was investigated, in order to better understand the thermal characteristics of UHIs.

2. Materials and Method

2.1 Materials

During summer 2023 air temperature data were acquired with the MetroTracker© device, a low-cost mini-meteorological station, designed by the Italian company Topon srl, for dynamic measurements, based on a patented RECS (Radiation Error Correction System) technology. It is connected with a smartphone application and a cloud-based infrastructure (https://MeteoTracker.com) that implements a global mobile meteorological network (Antoniciello, 2021). In a study conducted by Zanetti et al. (2023) the MeteoTracker© device was tested against a calibrated Lutron TM-947SD thermometer and it was found that the mobile device is reliable in measuring temperature values in dynamic conditions, with an accuracy of 0.1 °C. On the other hand, it is unable to detect temperature changes when not moving.
The MeteoTracker© device was used for 26 days of air temperature surveys conducted between July and September 2023. The device was installed to the handlebars of the bicycle or on the roof of the car, respectively for the afternoon (5pm) and night surveys (10pm) (Fig. 1).
For the comparison between air temperature and land use, the Corine Land Cover (CLC) database was used, and reclassified in order to obtain a geodatabase with only permeable and impermeable surfaces.

Figure 1. Meteotracker© installation on a bike and on a car

To develop the comparative analysis between the data collected by the MeteoTracker© device, the LST parameter and the NDVI index, bands 4,5 and 10 of satellites Landsat 8-9 were processed.
The analysis of the spatial data and the cartographic representation of the results were performed with QGIS 3.28 "Firenze" geographical analysis software, while Microsoft Excel© software was used for the processing of the statistical models. Google Earth Pro© software was used for the cartographic representation of the study areas.

2.2 Methods

In this section we briefly present the methodologies adopted for the identification UHI and the relations between air temperature, land cover, NDVI and LST. Detailed methodology workflow is presented in the Appendix.

2.2.1 Study Area: The study area is in the municipality of Padua, a city with 220.000 residents located in the North-East Italy, characterised by almost 50% of soil sealed. During the air temperature surveys, three different study areas were considered depending on the time of temperature measurement via mobile mapping, as shown in Figure 2. Study areas were delineated to encompass various land use types within their boundaries.

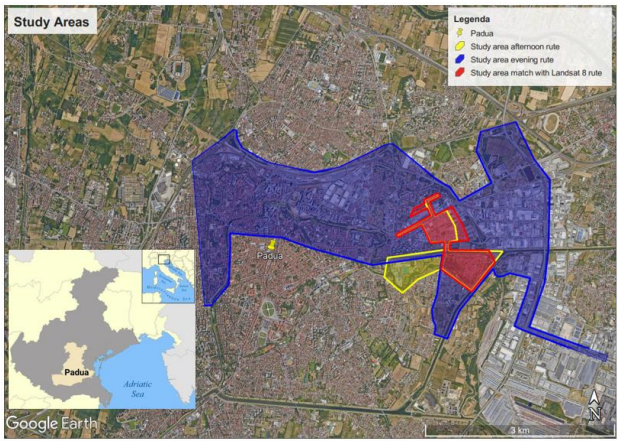

Figure 2. Study area for the different surveys. Satellite basemap: Google Earth Pro

2.2.2 Air Temperature Spatial Analysis: Air temperature records collected by Meteotracker© were averaged - for afternoon and night surveys separately - in a regular hexagonal fishnet (20x20 m) by using the "zonal statistics" tool in QGIS. Only hexagons with 26 records or more (at least equal of the days of the survey campaign) were taken into consideration. This method allows to identify the areas with higher temperature on average in the afternoon and at night in summer 2023 in Padua.

2.2.3 Satellite Data Analysis: In this study Landsat 8-9 images were elaborated in order to get two indexes: LST and NDVI. LST values are calculated by combining bands 4 (red), 5 (near-infrared) and 10 (thermal) from Landsat 8-9 as described in the Landsat Surface Temperature Product Guide (Zanter, 2018). NDVI is calculated from Landsat 8-9 bands 4 and 5 as described by Zanter (2018). The outcomes of these calculations yield two raster maps at a resolution of 30x30m, providing information on surface temperature and vegetation vigour within the municipality of Padua (Todeschi et al., 2022; Pappalardo et al., 2023).

2.2.4 Air Temperature and Land Cover: To better identify the role of vegetated impermeable surfaces in air temperature reduction, we analysed the distribution of temperature records for permeable and impermeable land use classes of CLC layer - both for afternoon and night datasets - by creating a violin plot chart. To continuously model the relationship between vegetation and air temperature, we conducted Ordinary Least Squares (OLS) modelling, correlating each air temperature record with the corresponding NDVI value of the pixel where the temperature was measured.

2.2.5 Air Temperature and LST: Many authors investigated the correlation between air temperature and LST (Zhang et al., 2014; Tajfar et al., 2020; Urban et al., 2013), but none of them used a spatially continuous dataset of survey. In this study we surveyed with MeteoTracker© the air temperature approximately 15 minutes before and 15 minutes after the Landsat 8 satellite image acquisition in Padua, the 8th of September at 11 am CET. Moreover, we investigated the correlation between air temperature and LST by using an OLS model, similarly as previously described for NDVI and air temperature.

3. Results

3.1 Air Temperature and Land Cover Relationship

The surveys conducted using MeteoTracker© yielded a geodatabase comprising sampled points covering a total distance of 540 km, over 26 days. Each afternoon, the same route was surveyed for geospatial data collection, with an extended route taken during night sessions. In Figure 3, the air temperature values for the afternoon of August 25, 2023, in both permeable and impermeable areas within a section of the city of Padua are depicted, while Figure 4 displays the corresponding values for the night.

Figure 3: Air temperature (°C) and land cover in the city of Padua registered the 25th August 2023, from 5.15 pm to 5.56 pm

Figure 4: Air temperature (°C) and land cover in the city of Padua registered the 25th August 2023, from 10.15 pm to 11.03 pm

It is possible to notice that the temperature values registered in permeable surfaces are in general lower than in the impermeable ones. In some densely anthropized areas, temperature can reach 35 °C during the afternoon and 29 °C during the night, while in vegetated areas and in proximity of the rivers, the temperature is significantly lower, with 31.6 °C in the afternoon and 26.3 °C in the night.

The violin plot in Figure 5 illustrates the distribution of all temperature values sampled during both afternoon and night sessions throughout the 26-day campaign. The data is segmented based on the land cover, distinguishing between permeable and impermeable surfaces. The findings indicate that impermeable areas are, on average, nearly 1 °C warmer than permeable ones, across both afternoon and night samplings.

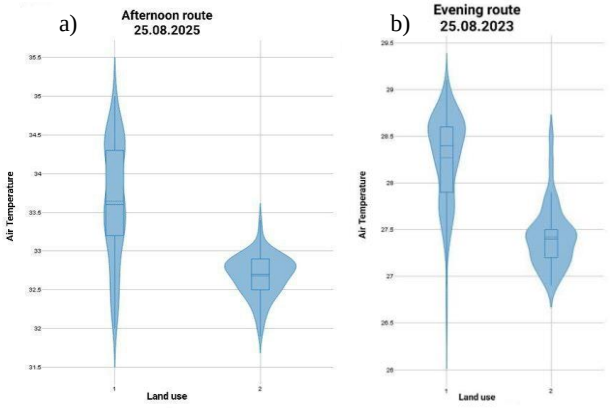

Figure 5: Violin plot of air temperature (°C) sampled in different land use areas (1= impermeable; 2= permeable) in all the 26 days of survey in summer 2023, during afternoon (a) and night (b).

3.2 Air Temperature and NDVI Relationship

To better understand the relationships between air temperature and the vegetation, the sampling areas of both afternoon and night routes were gridded with a hexagonal fishnet as described in section 2.2.2. For each hexagon the average temperature and the average NDVI values were calculated, as shown in figure 6 and 7 for the afternoon and night respectively.

Figure 6: Hexagonal fishnet (20x20 m) with average air temperature sampled during the afternoons of 26 days in summer 2023 in Padua and average NDVI value.

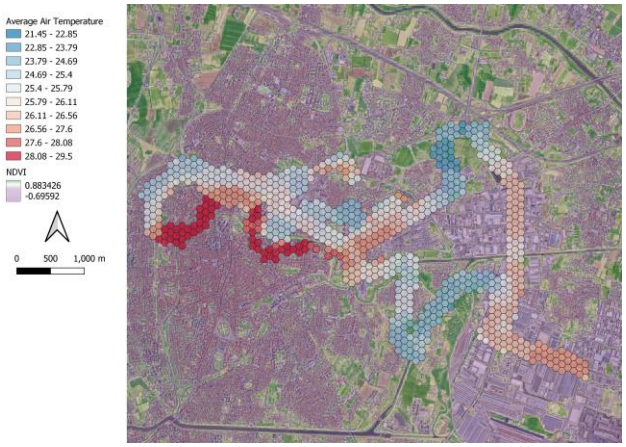

Figure 7: Hexagonal fishnet (20x20 m) with average air temperature sampled during the nights of 26 days in summer 2023 in Padua and average NDVI value.

The OLS regression models describe a negative correlation between air temperature and NDVI. During the afternoon, the regression coefficient indicates a reduction of 0.23 °C in air temperature for every 0.1 increase in NDVI, with an R^2 of 0.5 and $\alpha<0.005$ (Fig 8). During the night the regression coefficient is even higher, indicating a reduction of 0.3 °C in air temperature for every 0.1 increase in NDVI (Fig. 9), due to the thermal proprieties of impermeable materials such as asphalt.

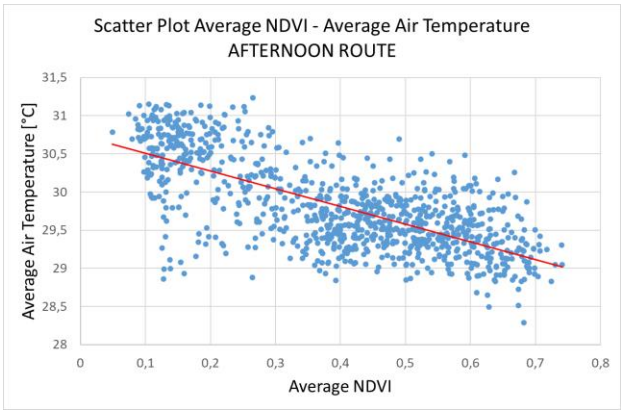

Figure 8: Scatterplot of air temperatures in the afternoons during 26 days survey in summer 2023 and NDVI of the sampling points, with OLS regression line in red.

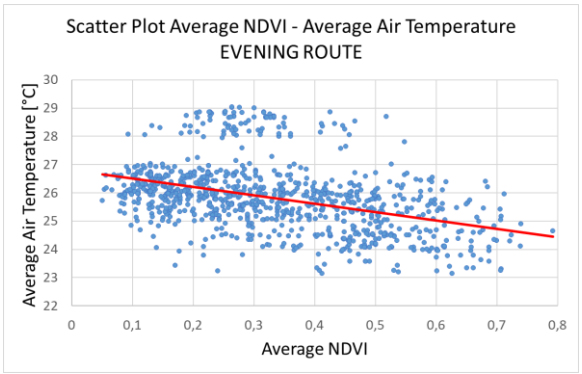

Figure 9: Scatterplot of air temperatures in the nights during 26 days survey in summer 2023 and NDVI of the sampling points, with OLS regression line in red.

3.3 Air Temperature and LST Relationship

Air temperature and LST seems to be strictly related, as shown in figure 10, in which air temperature is surveyed during the Landsat 8 image acquisition the 8th of September 2023. As for the NDVI, the areas close to the river and more vegetated have a lower LST value and also a lower air temperature.

Figure 10: Land surface temperature and air temperature the 8th of September during Landsat 8 acquisition at 11 am CET.

The OLS regression model between LST and air temperature indicates that there is a positive correlation, with an average increase of 0.5 °C in air temperature for every increase of 1 °C in LST (Fig 11). The R^2 of the OLS model is 0.27, with $\alpha<0.05$.

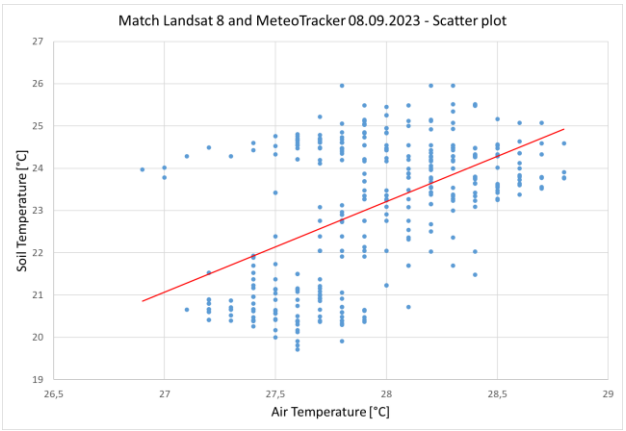

Figure 11: Scatterplot of air temperatures and LST temperature the 8th of September during Landsat 8 acquisition at 11 am CET

This result is a preliminary test that allows further investigation: a citizen science initiative to survey air temperature during Landsat 8 passages can increase the spatial surveyed area and therefore give more opportunity to model the relationship between air temperature, LST and land cover.

4. Conclusions

Following the considerations made regarding the different measurements and processing, it can be stated that the highest and coldest temperatures were always identified in the same areas, both during the night sessions and during the daytime measurements. Notably, highest temperatures are consistently found in the impervious areas of the city, whereas lower thermal conditions are associated with suburbs, cultivated fields, waterways, and parks. However, exceptions occur during morning measurements, attributed to tree-lined roads mitigating air temperature due to their cooling effect. NDVI analysis reveals that areas with sparse vegetation exhibit higher temperatures.

The presence of parks, green spaces, crops, and waterways significantly contributes to temperature reduction, especially in the afternoon. Moreover, nighttime temperature decreases are more pronounced in areas with higher NDVI, while they are less significant in high-sealed areas, attributed to thermal radiation from impermeable surfaces.

The correlation discovered between air temperature and land surface temperature could be further explored by augmenting data acquisition through low-cost mobile sensors, engaging citizen volunteers in citizen science initiatives. This participation not only fosters awareness and understanding of the phenomenon and its impacts but also facilitates a more comprehensive understanding of its health implications for citizens. By generating a robust database of air temperature throughout the city, such initiatives are crucial for prioritizing adaptation strategies and comprehending the effectiveness of nature-based solutions in enhancing thermal comfort measures.

Acknowledgements

This research project is part of the BRE.A.T.HE. (BREathing urbAn climaTe for HEalth) project funded by University of Padua – Innovative Students Projects. The financial support provided enabled us to conduct data collection, analysis, and interpretation, as well as cover expenses related to research materials, participant recruitment, and travel, where applicable. The PhD scholarship of the first author is funded by PNRR – Next Generation EU.

References

Antoniciello, G., 2021: MeteoTracker, piccola ma promettente stazione meteo portatile. *Nimbus*, 86, pp. 6-9.

Ballester, J., Quijal-Zamorano, M., Méndez Turrubiates, R.F., Pegenaute, F., Herrmann, F.R., Robine, J.M., Basagaña, X., Tonne, C., Antó, J.M. and Achebak, H., 2023. Heat-related mortality in Europe during the summer of 2022. *Nature medicine*, *29*(7), pp.1857-1866.

Dickinson, J.L., Zuckerberg, B. and Bonter, D.N., 2010. Citizen science as an ecological research tool: challenges and benefits. *Annual review of ecology, evolution, and systematics*, *41*, pp.149-172.

Giannopoulou, K., Santamouris, M., Livada, I., Georgakis, C. and Caouris, Y., 2010. The impact of canyon geometry on intra urban and urban: suburban night temperature differences under warm weather conditions. *Pure and applied geophysics*, *167*, pp.1433-1449.

Grigoraș, G. and Urițescu, B., 2019. Land use/land cover changes dynamics and their effects on surface urban heat island in Bucharest, Romania. *International Journal of Applied Earth Observation and Geoinformation*, *80*, pp.115-126.

IPCC, 2023. "AR6 Synthesis Report: Climate Change 2023". https://www.ipcc.ch/report/ar6/syr/

Koko, A.F., Yue, W., Abubakar, G.A., Alabsi, A.A.N. and Hamed, R., 2021. Spatiotemporal influence of land use/land cover change dynamics on surface urban heat island: A case study of Abuja metropolis, Nigeria. *ISPRS International Journal of Geo-Information*, *10*(5), p.272.

Morini, E., Touchaei, A.G., Rossi, F., Cotana, F. and Akbari, H., 2018. Evaluation of albedo enhancement to mitigate impacts of urban heat island in Rome (Italy) using WRF meteorological model. *Urban Climate*, *24*, pp.551-566.

Oke, T.R., 1973. City size and the urban heat island. *Atmospheric Environment (1967)*, *7*(8), pp.769-779.

Pappalardo, S.E., Zanetti, C. and Todeschi, V., 2023. Mapping urban heat islands and heat-related risk during heat waves from a climate justice perspective: A case study in the municipality of Padua (Italy) for inclusive adaptation policies. *Landscape and Urban Planning*, *238*, p.104831.

Robine, J.M., Cheung, S.L.K., Le Roy, S., Van Oyen, H., Griffiths, C., Michel, J.P. and Herrmann, F.R., 2008. Death toll exceeded 70,000 in Europe during the summer of 2003. Comptes rendus biologies, 331(2), pp.171-178.

Robinson, L.D., Cawthray, J.L., West, S.E., Bonn, A. and Ansine, J., 2018. Ten principles of citizen science. In *Citizen science: Innovation in open science, society and policy* (pp. 27-40). UCL Press.

Rousi, E., Kornhuber, K., Beobide-Arsuaga, G., Luo, F. and Coumou, D., 2022. Accelerated western European heatwave trends linked to more-persistent double jets over Eurasia. *Nature communications*, *13*(1), p.3851.

Rubio-Iglesias, J.M., Edovald, T., Grew, R., Kark, T., Kideys, A.E., Peltola, T. and Volten, H., 2020. Citizen science and environmental protection agencies: Engaging citizens to address key environmental challenges. Frontiers in Climate, 2, p.600998.

Tajfar, E., Bateni, S.M., Lakshmi, V. and Ek, M., 2020. Estimation of surface heat fluxes via variational assimilation of land surface temperature, air temperature and specific humidity into a coupled land surface-atmospheric boundary layer model. *Journal of Hydrology*, *583*, p.124577.

Todeschi, V., Pappalardo, S.E., Zanetti, C., Peroni, F. and Marchi, M.D., 2022. Climate Justice in the City: Mapping Heat-Related Risk for Climate Change Mitigation of the Urban and Peri-Urban Area of Padua (Italy). *ISPRS International Journal of Geo-Information*, *11*(9), p.490.

UN (2019), "World Urbanization Prospects. The 2018 Revision".
https://population.un.org/wup/Publications/Files/WUP2018-Report.pdf

Urban, M., Eberle, J., Hüttich, C., Schmullius, C. and Herold, M., 2013. Comparison of satellite-derived land surface temperature and air temperature from meteorological stations on the pan-Arctic Scale. *Remote Sensing*, *5*(5), pp.2348-2367.

Zanetti, C., Carraro, M., De Marchi, M. and Pappalardo, S.E., 2023. Volunteered Geographic Information for Mapping Urban Climate and Air Quality: Testing and Assessing 'Sniffer Bikes' with Low-Cost Sensors. *The International Archives of the Photogrammetry, Remote Sensing and Spatial Information Sciences*, *48*, pp.555-561.

Zanter, K., 2018: "Landsat surface temperature (ST) product guide."

Zhang, P., Bounoua, L., Imhoff, M.L., Wolfe, R.E. and Thome, K., 2014. Comparison of MODIS land surface temperature and air temperature over the continental USA meteorological stations. *Canadian Journal of Remote Sensing*, *40*(2), pp.110-122.

Appendix

The objective of the following appendix is to provide a condensed overview of the procedures undertaken to analyse the relationship between air temperature, land use, and NDVI. The workflow identified in Figure 12 is summarized as follows:

1. Importing MeteoTracker© measurements in CSV format, the Land Cover shapefile (CLC) of Padua municipality, and raw raster files of bands 4, 5, and 10 from Landsat 8 (collection 2 level 1) into QGIS.
2. Clipping bands 4, 5, and 10 with a 15 km buffer from Padua municipality's centroid, in order to get a smaller area.
3. Calculating the NDVI index using the method outlined by Pappalardo et al. (2023) with satellite data cropped in step 2.
4. Modifying the symbology of NDVI representation to visually distinguish value changes by categorizing ground conditions into 10 classes based on quantile values and assigning unique colors from purple to green via white.
5. Visualizing temperature points detected by the MeteoTracker© device, with a graduated color symbology from blue to red, divided into 10 class representing the deciles of the distribution.
6. Eliminating the initial minute of measurements from each route to mitigate device adaptation errors.
7. Generating a fishnet of hexagons of 20 m for afternoon routes and 100 m for evening routes.
8. Computing the average NDVI for each grid hexagon using the "zonal statistics" function within QGIS Processing tools.
9. Calculating route statistics (average, minimum, maximum, interval) for each grid hexagon using the same "zonal statistics" function, subsequently eliminating components with zero values. This step is repeated for each MeteoTracker© files.
10. Merging the results obtained in point 9 using the "vector merge" function, grouping files from afternoon and evening sessions separately.
11. Calculating the average temperature for each hexagon belonging to the grid, based on the fusion obtained in point 10. Components with zero values are eliminated.
12. Cleaning anomalies: eliminating figures containing less than twenty-six points for afternoon measurements and less than seven points for nighttime measurements to ensure coverage across all analysis sessions.
13. Merging individual MeteoTracker© routes using the "vector background" function, grouping afternoon and evening measurements separately.
14. Calculating statistics for the merged file obtained in point 13 (average, minimum, maximum, interval) for each hexagon, subsequently eliminating components with zero values.
15. Overlapping the fishnet containing the average NDVI index with that obtained in point 12, removing components with null values.
16. Overlapping the fishnet containing statistics of air temperature in each hexagon (file from point 14) with the Land cover map Map.
17. Creating a Scatter Plot graph from the intersection obtained in point 15, with average NDVI and average air temperature using Microsoft Excel.

18. Running an Ordinary Least Squares (OLS) model using the intersection obtained in point 15 through Microsoft Excel's "regression" tool.
19. Generating a Violin Plot from the intersection obtained in point 16, employing the QGIS DataPloty Plugin.

The same process employed for analysing the relationship between NDVI and air temperature can be adapted for the analysis of LST and its relationship with air temperature.

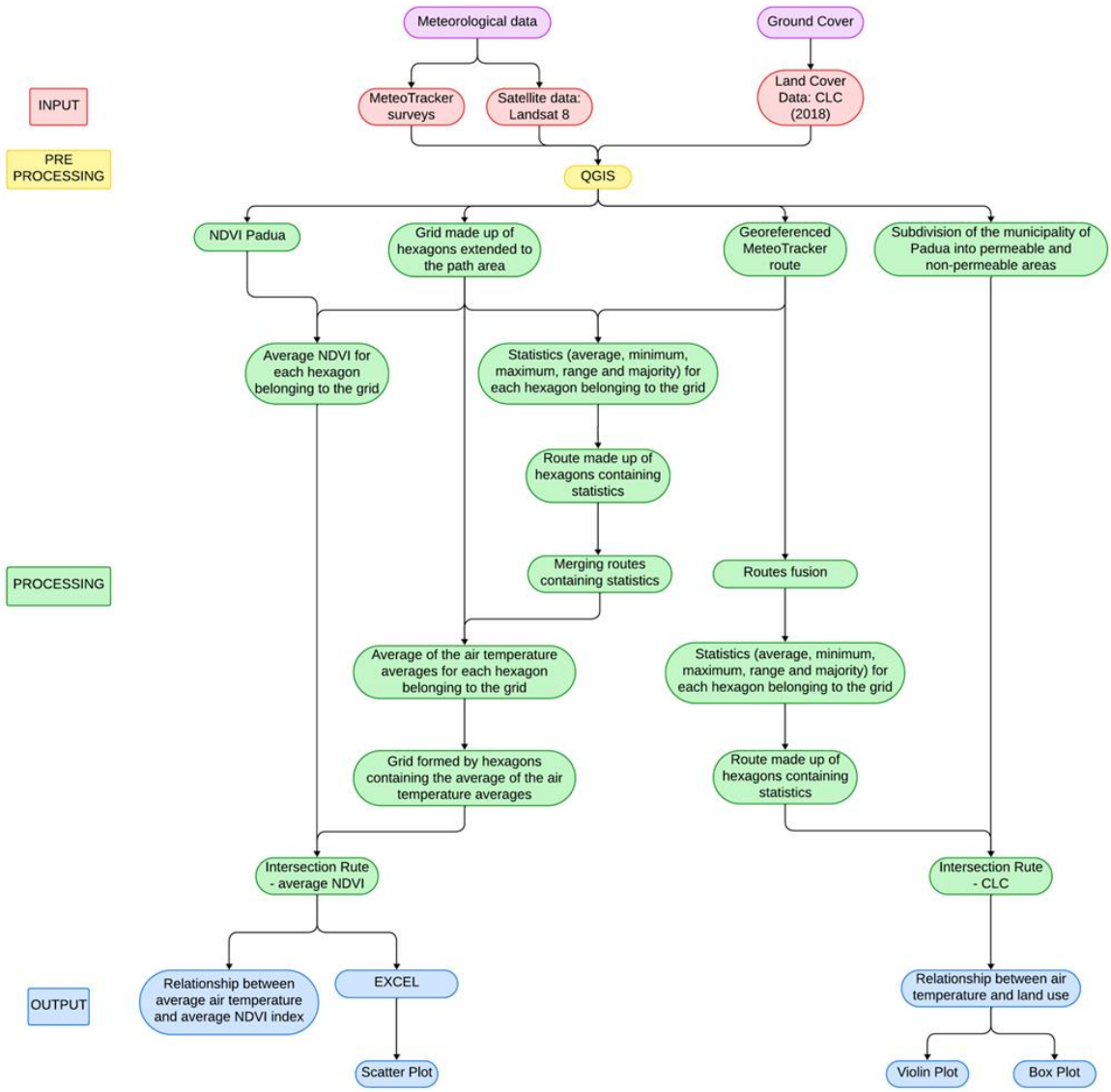

Figure 12: Methodological Workflow